Food Science and Technology Research, **21** (3), 365−370, 2015

doi: 10.3136/fstr.21.365

http://www.jsfst.or.jp

Original paper

Inactivation Characteristics and Modeling of Mold Spores by UV-C Radiation Based on Irradiation Dose

Vipavee Trivittayasil[1], Kohei Nashiro[1], Fumihiko Tanaka[2*], Daisuke Hamanaka[2] and Toshitaka Uchino[2]

[1]*Graduate School of Bioresource and Bioenvironmental Sciences, Kyushu University, 6-10-1, Hakozaki, Higashi-ku, Fukuoka 812-8581, Japan*

[2]*Laboratory of Postharvest Science, Faculty of Agriculture, Kyushu University, 6-10-1, Hakozaki, Higashi-ku, Fukuoka 812-8581, Japan*

Received August 31, 2014 ; Accepted January 13, 2015

Inactivation characteristics by UV-C radiation of *Cladosporium cladosporioides* and *Penicillium digitatum*, known as decay-inducing molds on fruits, were investigated. The survival curve of *C. cladosporioides* with irradiation dose was found to be biphasic in nature; the inactivation rate was initially high and slowed with increasing irradiation dose. In contrast, the survival curve of *P. digitatum* was approximately linear. A shoulder on the survival curves of both species was observed at low dose, indicating their resistance to low-dose UV-C. The mathematical model representing the inactivation of *C. cladosporioides* was the biphasic linear model, whereas the first-order kinetics model was applicable to *P. digitatum*.

Keywords: UV-C, mold, inactivation model, computational fluids dynamics

Introduction

Fresh or minimally-processed fruits are part of the standard diets of people throughout the world. The highly perishable nature of fruits necessitates proper postharvest treatment to preserve the freshness and quality. One measure to preserve fruit freshness is surface decontamination treatment. This treatment is applied to reduce the number of decay-inducing molds present on fruit surfaces. Microorganisms left untreated may multiply during the distribution process, leading to economic losses from product deterioration. There are many types of surface decontamination techniques. The disinfection treatments currently in use for inactivating microorganisms on fresh agricultural produce typically involve chemicals (Beuchat, 1998). However, due to growing concerns regarding the effects of chemical residues on human health, alternative physical techniques such as UV-C irradiation have been receiving attention in recent years.

UV-C radiation employs a wavelength range of 100 − 280 nm and exerts high germicidal activity. Inactivation by UV-C is based on nucleic acid damage to the cell or virus (Hijnen *et al*., 2006). Many studies on the effects of UV-C have involved agricultural produce such as citrus fruit (Ben-yehoshua *et al*., 1992), grapefruit (Droby *et al*., 1993), peach (Stevens *et al*., 1998), strawberry (Marquenie *et al*., 2003), tomato (Liu, 1993), pepper (Vicente *et al*., 2005) and spinach (Escalona *et al*., 2010). UV-C was found to have an inactivation effect and the ability to induce resistance (Terry & Joyce, 2004). Thus, it has been difficult to determine optimal treatment conditions when two effects interact with one another. This has encouraged researchers to independently find the optimal treatment intensity for each fruit under various specific conditions, such as the timing of inoculation and defined sets of radiation intensity and time. However, this approach might be too time-consuming or specific to be used in broader applications. Thus, inactivation models should be constructed with common decay-inducing molds as one of the optimization tools for

*To whom correspondence should be addressed. E-mail: fumit@bpes.kyushu-u.ac.jp

determining appropriate UV-C treatment levels.

The aim of this study is to investigate the inactivation characteristics of mold spores responsible for fruit decay. The presence of mold spores on fruit surfaces was simulated *in vitro* by spreading a solution containing mold spores onto solid nutrient agar. Various inactivation models, which can describe the phenomenon, were investigated.

Materials and Methods

Preparation of samples *Cladosporium cladosporioides* NBRC 30313 and *Penicillium digitatum* NBRC 33116 were obtained from NITE Biological Resource Center (Chiba, Japan). Fungal spores were harvested by washing the culture with rehydration fluid and the obtained solution was transferred onto potato dextrose medium (PDA; NISSUI Pharmaceutical Co., Ltd, Japan). The fungi were grown at 25℃ for 7 days. The spores were harvested using a distilled water and detergent solution (ca. 1 mL/L Tween80). A spreader was used to gently scrap the spores from the agar surface into suspension. As the obtained suspension contained both mycelia and spores, it was filtered through a funnel filled with glass wool to remove the mycelial fragments and washed by centrifuging three times for 10 min, at 20℃ and 1510 ×*g*. The detergent was replaced with distilled water and the original suspension was adjusted to 10^7 CFU mL^{-1} by measurement of optical density (OD = 1) at 600 nm. Different concentrations of the original solution were prepared and 0.1 mL of each dilution was transferred onto PDA agar plates. A spreader was used to distribute the solution evenly and the solution was allowed to dry for irradiation treatment.

UV-C treatment The UV-C equipment is shown in Fig. 1. The lamp (*GL6*; Toshiba, Japan) was turned on for at least 3 minutes before the experiment to allow the lamp intensity to stabilize. The radiation distance from the base of the lamp to the surface of the agar was 50, 100, 150 and 200 mm. After the radiation treatment, samples were incubated at 25℃ for three days before counting the number of visible colonies (CFU). The maximum treatment time was 30 minutes.

Prediction models

a) First order kinetic model

Microbial mortality has been treated as a process that follows first-order kinetics. The first order kinetic model is a one-parameter model that assumes all cells in a population have an identical resistance to a lethal treatment and the logarithm of the number of survivors declines linearly over treatment time.

$$\frac{dN(t)}{dt} = -kN(t) \quad \cdots\cdots \text{Eq. 1}$$

Integrating Eq. (1) will give

$$N(t) = N_0 \exp(-kt) \quad \cdots\cdots \text{Eq. 2}$$

or

$$\log_{10}\frac{N}{N_0} = -\frac{kt}{2.303} \quad \cdots\cdots \text{Eq. 3}$$

where N is the number of surviving microorganisms (CFU mL^{-1}), N_0 is the initial number of microorganisms (CFU mL^{-1}), k is the inactivation rate constant (s^{-1}) and t is the treatment time (s). The kinetics of microbial inactivation by UV-C is a function of UV dose, expressed as the product of radiation intensity and exposure time. To investigate the inactivation effect based on irradiation dose, the average irradiation intensity was incorporated into the equation as follows,

$$\log_{10}\frac{N}{N_0} = -\frac{k'It}{2.303} \quad \cdots\cdots \text{Eq. 4}$$

where I is the average irradiation intensity on an agar (kW m^{-2}) and k' is the modified inactivation rate constant (m^2 kJ^{-1}).

b) Weibull model

The two-parameter model is based on the assumption that cells in a population have different resistance and the resistance to a stress follows a Weibull distribution (Bialka *et al*., 2008).

$$\log_{10}\frac{N}{N_0} = -\frac{1}{2.303}\left(\frac{t}{\alpha}\right)^{\beta} \quad \cdots\cdots \text{Eq. 5}$$

where α is the characteristic time (s) and β is the shape factor. The β value determines the shape of a survival curve; if $\beta > 1$ then the survival curve has a downward concavity, and if $\beta > 1$ the survival curve has an upward concavity. The equation was rearranged as follows,

$$\log_{10}\frac{N}{N_0} = -\frac{1}{2.303}\left(\frac{It}{\alpha}\right)^{\beta} \quad \cdots\cdots \text{Eq. 6}$$

where α' is the modified characteristic coefficient (kJ m^{-2}).

c) Biphasic linear model

The three-parameter model assumes that the population is split into two populations; one treatment-sensitive and the other treatment-resistant.

$$\log_{10}\frac{N}{N_0} = \log_{10}\left[(1-f)\cdot 10^{-\frac{t}{D_{sens}}} + f\cdot 10^{-\frac{t}{D_{sens}}}\right] \quad \cdots\cdots \text{Eq. 7}$$

where (1-f) and f are the fraction of treatment-sensitive and treatment-resistant populations, with D value of D_{sens} (s) and D_{res} (s), respectively. D value is the time required for one log reduction in the number of microorganisms. The equation was rearranged as follows,

$$\log_{10}\frac{N}{N_0} = \log_{10}\left[(1-f)\cdot 10^{-\frac{t}{D'_{sens}}} + f\cdot 10^{-\frac{t}{D'_{sens}}}\right] \quad \cdots\cdots \text{Eq. 8}$$

where D'_{sens} and D'_{sens} is the modified D_{sens} (kJ m^{-2}) and D_{res} (kJ m^{-2}), respectively.

Least squares method The inactivation parameters in the

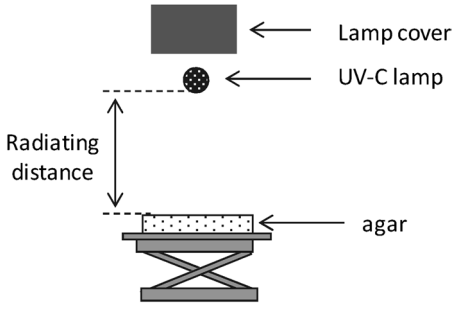

Fig. 1. Schematic of the irradiation set-up

inactivation prediction models can be obtained by the least squares method. The purpose of the least squares method is to determine the inactivation parameters that can minimize the sum of squared residuals. A residual is defined as the difference between the actual value of the dependent variable, which is the experimental data, and the value predicted by the model. The sum of squared residuals can be calculated as follows,

$$S = \sum \left[\left(\log \frac{N}{N_0} \right)_{\text{pre}} - \left(\log \frac{N}{N_0} \right)_{\text{exp}} \right]^2 \quad \cdots\cdots \text{Eq. 9}$$

Model evaluation Triplicate treatments were carried out. The model evaluation was performed using root mean square error (RMSE) and coefficient of determination (R^2). RMSE can be computed using the predicted (pre) and experimental (exp) logarithmic reductions by the following equation.

$$\text{RMSE} = \sqrt{\frac{1}{n} \sum \left[\left(\log \frac{N}{N_0} \right)_{\text{pre}} - \left(\log \frac{N}{N_0} \right)_{\text{exp}} \right]^2} \quad \cdots\cdots \text{Eq. 10}$$

Lower RMSE values indicate better fit. In addition, adjusted coefficient of determination $\overline{R}^2$is used to evaluate goodness-of-fit of the model.

$$\overline{R}^2 = 1 - (1 - R^2) \frac{n-1}{n-p-1} \quad \cdots\cdots \text{Eq. 11}$$

Where R^2 = 1 - (RSS/TSS), p is the total number of explanatory variables, n is the sample size, RSS is the residual sum of squares and TSS is the total sum of squares. $\overline{R}^2$is used instead of R^2 because it helps to correct for different numbers of explanatory terms in different models.

Calculation of average irradiation intensity on agar Average irradiation intensity on the upper surface of the agar was calculated using the computational fluid dynamics (CFD) method. CFD was employed because it is difficult to determine average irradiation intensity by UV meter, which can only measure UV rays coming from a specific direction. CFD is useful in simulating conditions where detailed measurements are hard to obtain (Xia & Sun, 2002). The CFD simulation steps included creating geometry and mesh, setting model parameters and obtaining post-calculation results. The geometry creation was performed in DesignModeler 13.0 (ANSYS, Pennsylvania**,** USA). The geometry was created based on an actual UV-C lamp, cover and agar plate. Four geometries were produced for each radiation distance (50, 100, 150 and 200 mm). The geometries were then imported into ANSYS Meshing (ANSYS) to create a volume mesh. The inflation was applied to the domain faces of the lamp, cover and medium agar. The inflation helps to refine the mesh in those regions. The resulting numbers of mesh elements were 474082, 484481, 488254 and 486850 for the 50, 100, 150 and 200 mm geometries, respectively. The simulation was carried out in Fluent software version 13.0 (ANSYS) employing the discrete ordinates radiation model to solve the radiative transfer equation in the computational domain using a solid angle discretization, with theta and phi division of 10x10. The emissivity for the UV-C lamp, cover and agar were 0.89 (Coussirat *et al*., 2008), 0.04 (Incropera & DeWitt, 2001) and 0.98 (Chatani, 2009), respectively. A diffuse fraction of 1 was assigned to the semi-transparent wall of the lamp sleeve and 0.5 to other walls. The governing continuity, momentum and energy equations for the laminar incompressible flow were solved for the defined geometries. There was no forced airflow and only natural convection was considered.

An input of UV lamp power was required for the simulation setting. As UV lamp power cannot be measured directly, it was estimated using CFD simulation by finding the UV power producing the same irradiation intensity as measured. The UV power of lamps used for *C. cladosporioides* and *P. digitatum* experiments was estimated to be 101.15 and 99.25 Wm^{-2}, respectively. All temperatures at the boundaries were initially set at 10 K to prevent calculation of other heat sources aside from the UV-lamp. A first order upwind discretization scheme was used to approximate the governing equation. The iteration number was 100.

Results and Discussion

Average irradiation intensity of UV-C The calculation of average irradiation intensity of UV-C on an agar plate was performed using CFD simulation. The average UV-C irradiation intensity on the agar plate is shown in Table 1. As indicated in the table, lamp 1 was used in the *C. cladosporioides* experiment and lamp 2 was used in the *P. digitatum* experiment.

Inactivation characteristics of mold spores by UV-C Figure 2 shows the surviving population of *C. cladosporioides* and *P. digitatum* relative to treatment time at different radiation distances. The survival curve of *C. cladosporioides* was an upward concavity. The inactivation patterns at all radiation distances showed a rapid initial decrease in the number of surviving spores during radiation treatment, which slowed after a certain threshold. For *P. digitatum*, the survival curve exhibited a linear decrease with treatment time. However, unlike *C. cladosporioides*, the tail was not clearly observed in this study.

For both mold species, a shoulder was observed at a radiation distance of 200 mm, which emits the lowest radiation intensity. Many studies have confirmed that homogeneous populations of organisms exhibit an initial resistance to UV light, in the form of a shouldered survival curve (Severin *et al*., 1983). The reason may be that microorganisms absorbing a sub-lethal UV dose may recover and continue multiplying (Ye *et al*., 2007). To observe the occurrence of a shoulder for decay-inducing microorganisms, the inactivation experiment of *C. cladosporioides* was conducted at longer radiation distances (Fig. 3). It was observed that the shoulder persisted to a certain irradiation dose; thus, it is possible that a sub-lethal dose exists. More studies are required to understand the phenomenon of the shoulder.

Emerick *et al*. (2000) suggested that high UV-C doses employed for typical wastewater disinfection usually tended to hide the initial resistance of specific bacterial species and strains. Thus, the need to

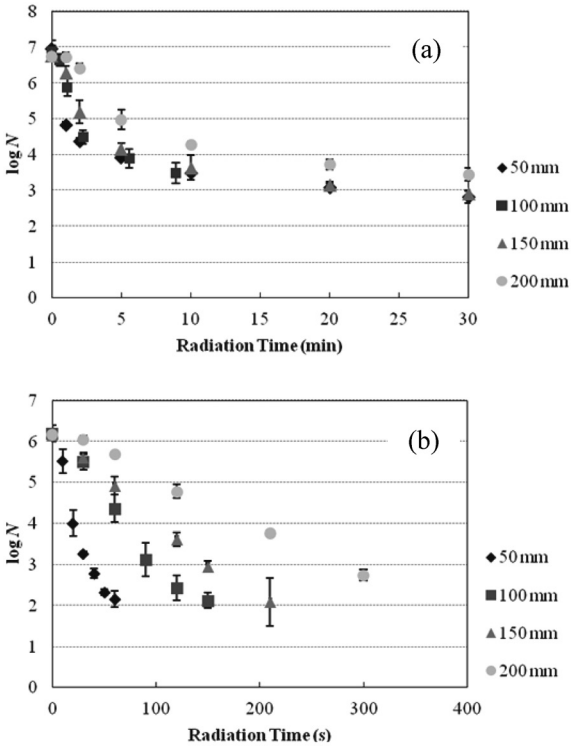

Fig. 2. Survival curves for *C. cladosporioides* (a) and *P. digitatum* (b) at different radiation distances

Table 1. Calculated average irradiation intensity on agar

Radiation distance (mm)	Average irradiation intensity on agar (W m^{-2})	
	Lamp 1*	Lamp 2*
50	13.8	13.2
100	6.61	6.38
150	3.72	3.64
200	2.13	2.29

* Lamp 1 was used for *C. cladosporioides* and lamp 2 was used for *P. digitatum*.

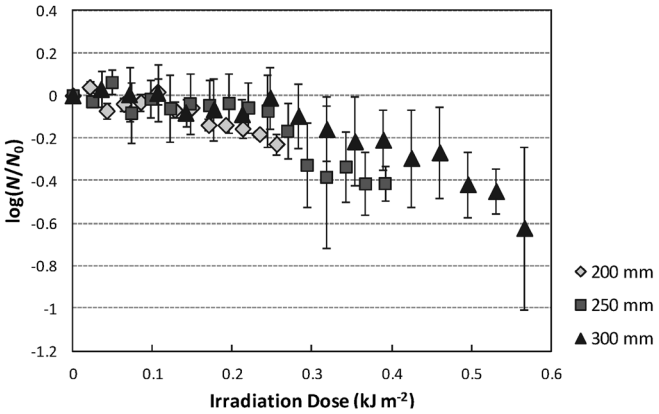

Fig. 3. Illustration of a shoulder effect for *C. cladosporioides*

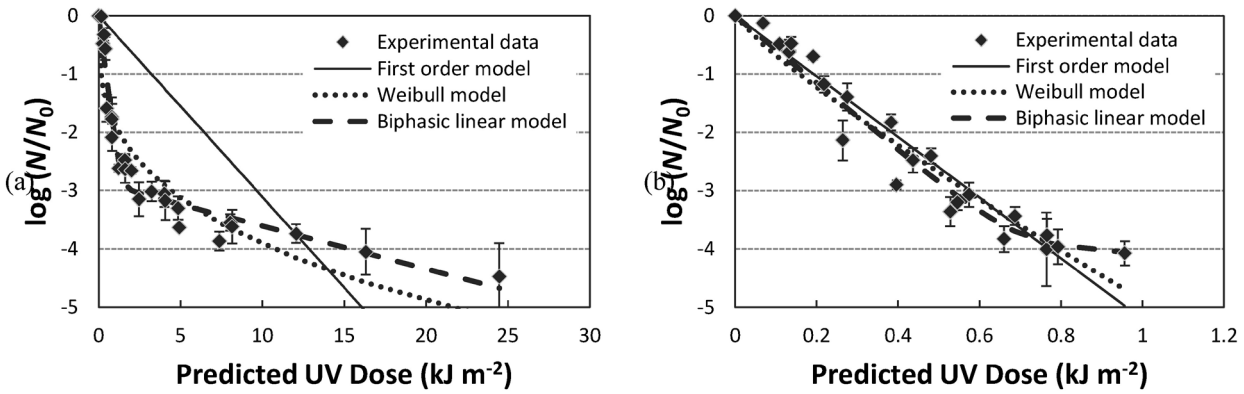

Fig. 4. Inactivation curves of (a) *C. cladosporioides* and (b) *P. digitatum* fitted to different prediction models

consider the effect of a shoulder will depend on the radiation intensity and dose required for surface decontamination techniques.

Prediction model The data of different radiation distances (50, 100, 150 and 200 mm) was combined and fitted with the prediction models using the least squares method (Fig. 4). The fitted parameters are shown in Table 2. For *C. cladosporioides*, the Weibull and biphasic linear models were found to fit well with the inactivation result, while the first order model failed to describe the inactivation due to the biphasic nature of the inactivation curve. The inactivation curve exhibited upward concavity, which can be interpreted to mean weak or sensitive members of the population are destroyed at a relatively fast rate, leaving behind survivors of higher and higher resistance (Peleg, 2000). Of all the models, the biphasic linear model was found to be the most accurate, with an $\overline{R}^2$ value of 0.96 and RMSE of 0.25 (Table 3).

The result suggested that the population of *C. cladosporioides* differs in resistance to UV-C, and can thus be categorized into weak and strong populations, following the assumption of the biphasic linear model. For *P. digitatum*, all three models accurately explained the inactivation phenomenon with high $\overline{R}^2$ value.

However, the good agreement between the experimental data and predictions does not prove which one is mechanistically correct. The inactivation curve of the experimental data was observed to be linear with radiation dose, which follows the assumption of the first order model that the entire population has the same resistance to a stress. The first order model was then

Table 2. Fitted parameters

Microorganism	First order model	Weibull model		Biphasic linear model		
	k' (m^2 kJ^{-1})	α' (kJ m^{-2})	β	f	D'_{sens} (kJ m^{-2})	D'_{res} (kJ m^{-2})
C. cladosporioides	0.72	0.011	0.323	0.00136	0.45	13.55
P. digitatum	11.98	0.060	0.859	0.00011	0.17	7.39

Table 3. Model assessment

Prediction model	Adjusted R^2		RMSE	
	C. cladosporioides	*P. digitatum*	*C. cladosporioides*	*P. digitatum*
First order model	−	0.92	−	0.38
Weibull model	0.84	0.93	0.50	0.35
Biphasic linear model	0.96	0.95	0.25	0.28

chosen as the most suitable model because it provided accurate prediction while being a simple model.

The low UV-C sensitivity of *C. cladosporioides* in comparison with *P. digitatum* could be related to melanin-like pigments. *C. cladosporioides* is characterized by pigmented mycelia and spores due to the presence of 1,8-dihydroxynaphthalene, a melanin-like compound (Llorente *et al*., 2012). Spores of melanized fungi have been found to have higher resistance against environmental stresses such as high temperature and UV-C radiation (Abbo, 2012). This could explain why *P. digitatum*, which is a non-melanized fungus, is significantly more sensitive to UV-C radiation.

Conclusion

The survival curves for UV-C treatment were observed to differ according to microbial type in terms of inactivation rate and shape. A common feature in *C. cladosporioides* and *P. digitatum* was the presence of a shoulder at low radiation intensity. The biphasic linear model could accurately describe the inactivation of *C. cladosporioides* by UV-C. For *P. digitatum*, all models could be used to describe the phenomenon; however, the first order model was deemed the most suitable due to the nature of the inactivation curve.

Acknowledgement This research was supported by the Ministry of Education, Science, Sports and Culture of Japan (Project No.22580289). We would like to sincerely thank Misaki Tsuru who was studying at Kyushu University for her invaluable help.

References

Abbo, A. S. H. (2012). The Dark Side of Fungal Melanin: *Alternaria alternata* as Example. Tropentag, Göttingen, Germany.

Ben-Yehoshua, S., Rodov, V., Kim, J. J., and Carmeli, S. (1992). Preformed and induced antifungal materials of citrus fruits in relation to the enhancement of decay resistance by heat and ultraviolet treatments. *J. Agric. Food. Chem.*, **40**, 1217-1221.

Beuchat, L. R. (1998). Surface decontamination of fruits and vegetables eaten raw: a review. Food Safety Unit, World Health Organization. pp. 42.

Bialka, K. L., Demirci, A., and Puri, V. M. (2008). Modeling the inactivation of *Escherichia coli* O157:H7 and *Salmonella enterica* on raspberries and strawberries resulting from exposure to ozone or pulsed UV-light. *J. Food Eng.*, **85**, 444-449.

Chatani, M. (2009). CFD simulation of the surface decontamination of fruits by infrared radiation heating. M. Sc. Thesis, Kyushu University, Fukuoka.

Coussirat, M., Guardo, A., Jou, E., Egusquiza, E., Cuerva, E., and Alavedra, P. (2008). Performance and influence of numerical sub-models on the CFD simulation of free and forced convection in double-glazed ventilated façades. *Energ. Buildings*, **40**, 1781-1789.

Droby, S., Chalutz, E., Horev, B., Cohen, L., Gaba, V., Wilson, C. L., and Wisniewski, M. (1993). Factors affecting UV-induced resistance in grapefruit against the green mould decay caused by *Penicillium digitatum*. *Plant Pathol.*, **42**, 418-424.

Emerick, R. W., Loge, F. J., Ginn, T., and Darby, J. L. (2000). Modeling the inactivation of particle-associated coliform bacteria. *Water Environ. Res.*, **72**, 432-438.

Escalona, V. H., Aguayo, E., Martínez-Hernández, G. B., and Artes, F. (2010). UV-C doses to reduce pathogen and spoilage bacterial growth in vitro and in baby spinach. *Postharvest Biol. Technol.*, **56**, 223-231.

Hijnen, W. A. M., Beerendonk, E. F., and Medema, G. J. (2006). Inactivation credit of UV radiation for viruses, bacteria and protozoan (oo)cysts in water: A review. *Water Res.*, **40**, 3-22.

Incropera, F. P. and DeWitt, D. P. (2001). "Fundamentals of Heat and Mass Transfer (5th ed.)". Asia: Wiley.

Liu, J., Stevens, C., Khan, V. A., Lu, J. Y., Wilson, C. L., Adeyeye, O., Kabwe, M. K., Pusey, P. L., Chalutz, E., Sultana, T., and Droby, S. (1993). Application of ultraviolet-C light on storage rots and ripening of tomatoes. *J. Food Prot.*, **56**, 868-873.

Llorente, C., Bárcena, A., Vera Bahima, J., Saparrat, M. C. N., Arambarri, A. M., Rozas, M. F., et al. (2012). *Cladosporium cladosporioides* LPSC 1088 produces the 1,8-dihydroxynaphthalene-melanin-like compound and carries a putative pks gene. *Mycopathologia*, **174**, 397-408.

Marquenie, D., Michiels, C. W., Van Impe, J. F., Schrevens, E., and Nicolai, B. N. (2003). Pulsed white light in combination with UV-C and

heat to reduce storage rot of strawberry. *Postharvest Biol. Technol.*, **28**, 455-461.

Peleg, M. (2000). Microbial survival curves — the reality of flat "shoulders" and absolute thermal death times. *Food Res. Int.*, **33**, 531-538.

Severin, B. F., Suidan, M. T., and Engelbrecht, R. S. (1983). Kinetic modeling of U.V. disinfection of water. *Water Res.*, **17**, 1669-1678.

Stevens, C., Khan, V. A., Lu, J. Y., Wilson, C. L., Pusey, P. L., Kabwe, M. K., Igwegbe, E. C. K., Chalutz, E., and Droby, S. (1998). The germicidal and hormetic effects of UV-C light on reducing brown rot disease and yeast microflora of peaches. *Crop Prot.*, **17**, 75-84.

Terry, L. A. and Joyce, D. C. (2004). Elicitors of induced disease resistance in postharvest horticultural crops: a brief review. *Postharvest Biol. Technol.*, **32**, 1-13.

Vicente, A. R., Pineda, C., Lemoine, L., Civello, P. M., Martinez, G. A., and Chaves, A. R. (2005). UV-C treatments reduce decay, retain quality and alleviate chilling injury in pepper. *Postharvest Biol. Technol.*, **35**, 69-78.

Xia, B. and Sun, D.-W. (2002). Applications of computational fluid dynamics (cfd) in the food industry: a review. *Comput. Electron Agr.*, **34**, 5-24.

Ye, Z., Koutchma, T., Pasiri, B., Larkin, J., and Forney, L. J. (2007). Ultraviolet inactivation kinetics of *Escherichia coli* and *Yersinia pseudotuberculosis* in annular reactors. *J. Food Sci.*, **72**, E271-E278.